# Slow Moving Target Detection for Airborne Radar Systems by Dynamic Programming on SAR Images

Gorkem GURER*†, Sencer KOC†, Cagatay CANDAN† and Umut ORGUNER†

*Radar and Electronic Warfare Systems Business Sector, ASELSAN, Ankara, Turkey
Email: ggurer@aselsan.com.tr

†Department of Electrical and Electronics Engineering, Middle East Technical University, Ankara, Turkey
Email: skoc,ccandan,umut@metu.edu.tr

*Abstract*—A dynamic programming based approach is proposed to detect slow moving, low reflectivity targets for airborne radar systems. The suggested method utilizes the reflectivity amplitudes of the SAR image, possibly containing multiple slow moving targets, and poses the target detection problem as a maximum likelihood sequence detection problem. Dynamic programming is applied to capture the target related features such as along track smeared target signatures in the SAR image to this aim. Typical clutter and target models are estimated from SAR images. The performance of the algorithm is illustrated on a real SAR image acquired with SARPER™ radar developed by ASELSAN.

## I. INTRODUCTION

Slow moving target detection is a challenging problem for airborne radar systems, typically for SAR/Ground Moving Target Indication (GMTI) systems. The problem is especially challenging for targets with small radar cross sections and low radial velocities such as dismounts, i.e., troops dismounting vehicles [1]. The approaches towards the solution of this problem mainly consist of two groups: SAR based and GMTI based approaches. SAR based approaches generally utilize the difference between multiple SAR images collected from the same scene in a short period of time [1], [2]. Ensuring the coherency of these images for the calculation of the difference image is an almost equally challenging problem. Some other approaches are based on focusing the response to a moving target with an assumed target phase history [3]. For GMTI based approaches, the radial target velocity of the dismount often falls below the minimum detectable velocity of the system. To overcome this problem a dismount motion model is incorporated with the Space Time Adaptive Processing (STAP) clutter suppression filter weights in [4]. As in every model based approach the mismatch of the assumed target model and the true target motion could result in high false alarm and/or miss rates. In this paper, we present an alternative approach based on sequence detection via dynamic programming. The approach is closely related with the dim target detection problem, a problem also known as track-before-detect (TBD) problem.

Our goal is to adapt the sequence detection problem, whose solution is obtained via dynamic programming in general, to the problem of interest. At the outset, we would like to remind that SAR images are constructed with the processing of raw data whose duration is orders of magnitude larger than a typical coherent processing interval (CPI) of a GMTI system. Hence, a SAR image can be considered to contain sufficiently large energy return from the target, which is, unfortunately, not localized due to the target motion. The main goal of the study is to treat the problem as a sequence detection problem and utilize the track-before-detect methods to extract the target signal from the real-valued SAR image.

Track Before Detect methods are used in order to utilize the raw target measurement information to the maximum extent to detect and track weak targets. Therefore, it can be anticipated that TBD algorithms are good solution candidates for the problem of slow moving target detection from a SAR image. Batch and recursive TBD studies such as particle filter based tracking [5], [6], [7], [8]; Hough transform based sea target tracking [9], [10] and dynamic programming (DP) based maneuvering target tracking [11], [12] can be found in the literature for the detection of low Signal to Interference Plus Noise Ratio (SINR) moving targets with infrared and optical sensors. References [11] and [12] employ the DP-TBD method to achieve better detection performance on maneuvering targets. Moving target signature appearing in a SAR image is analogous to a slow maneuvering target since the signature also extends in the cross track direction. Reference [13] studies DP based TBD problem for moving target detection on SAR images. The paper applies pre-processing to the SAR image by partitioning the raw data into sub-images and subtracting the adjacent ones to improve Signal to Clutter Ratio (SCR). Pre-processing also includes a Constant False Alarm Rate (CFAR) threshold. DP-TBD algorithm is then applied to the pre-processed data utilizing the fact that moving target signature in the SAR image shows the same characteristic between adjacent frames. Moving target in a SAR image has an along track smeared signature with similar pixel intensities forming a line-like signature. Therefore sub-images formed by partitioning the original SAR image have moving target signature pieces showing the similar smear and intensity characteristics. The results show that the DP-TBD method is a successful candidate to achieve low SCR moving target detection in SAR systems.

The proposed approach in this paper, different from [13], does not involve pre-processing of the SAR data to improve the SCR. Instead, the parameters of clutter probability density function (pdf) are estimated from the image data and the estimated pdf model is used to calculate the likelihood ratio

more accurately. In the proposed method, a high resolution SAR image is used where the along track (placed into the columns of the image matrix) and cross track (placed into the rows of the image matrix) directions correspond to time and position axes, respectively. Hence, we associate each radar scan in the conventional target tracking problem with a single column of the SAR image. With this association the trajectory of the target appears on consecutive columns.

The main issues with DP-TBD algorithm are the partitioning of the target space, heavy computational load and storing multiple scans of data for processing [14]. The advantages of using a SAR image that reduce these problems in DP-TBD algorithms are:

- The use of a SAR image eliminates the problem of storing processed data since all of the information from the target is already stored in the SAR image,
- As the resolution increases the clutter to target return ratio decreases,
- Smeared moving target signature shows similar pixel intensities throughout the target containing pixels.

## II. PROPOSED METHOD

In this section, we present the basics of dynamic programming in the context of a track-before-detect problem and then describe their application to the problem of interest.

### A. DP-TBD Algorithm Fundamentals

DP-TBD algorithm searches for the trajectory with the maximum score iteratively [15]. At each iteration, the path which maximizes the sum of the inherited score from the previous state and the state transition cost is chosen. A state transition cost is assigned to each allowed state transition. Maximization process is realized only for the allowable states at each frame which makes DP more computationally efficient than the exhaustive search. At the end of the search, detection is made by thresholding the scores of each cell. Once a detection is made, trajectories can be traced backwards from the stored optimum state transition values as the name "Track Before Detect" suggests [16].

The detailes of DP algorithm can be found in [16]. Here, we present only the end result. The recursive maximization is given as [16]:

$$LPR_k^*(j_k) = l_k(j_k) + \max_{j_{k-1}}[\log(p(j_k|j_{k-1})) + LPR_{k-1}^*(j_{k-1})]$$
(1)

$$l_k(j_k) = \log\left(\frac{p(Y_k|H_1, j_k)}{p(Y_k|H_0)}\right)$$
(2)

where $LPR$ stands for the log probability ratio, $k$ denotes time index and $j_k$ denotes the test cell at time $k$. $LPR_k^*(j_k)$ is the score of the candidate track. $l_k(j_k)$ is the log likelihood ratio of the target and the background intensity pdf models. The pdf $p(j_k|j_{k-1})$ represents the transition cost function [16]. $Y_k$ denotes the raw measurements (values of the SAR image pixels), $H_1$ and $H_0$ denote target present and target not present cases, respectively. The illustration of the terms in (1) on an image matrix with dimensions $M \times N$ is given in Fig.1. The

cell of interest is $LPR_k^*(3)$ whose allowed state transitions are within 2 pixels and denoted as $p(3|1:5)$. Target is declared
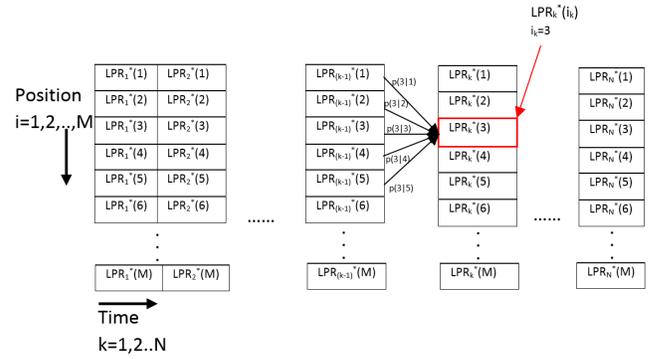


Fig. 1. Dynamic programming illustration on the image matrix.

when $LPR_k(j_k)$ score exceeds a threshold. Let the target state bins satisfying this criterion be shown as $j_{1:k}^*$. Operating only on $LPR_k^*(j_k)$ at each time index $k$ makes DP computationally efficient. Tracing back the target state trajectory is possible once a detection is made. The detection threshold is most commonly set by empirical methods. In this work, a detection is made by employing CFAR on the $LPR$ scores. Employing CFAR after TBD is also studied by [17] for dim moving target detection from a sequence of infrared images.

SAR images have speckled texture inherently. Log-probability-ratio, $LPR$, is more robust for implementation than the probability ratio in heavily speckled image due to finite precision arithmetic problems [16].

The DP-TBD algorithm is evaluated on real data collected from a manned platform carrying SARPER™ radar system. SARPER™ is an X band airborne radar system with slotted waveguide antenna [18]. Test image is a high resolution ($\ll$1 m) SAR image acquired at a range beyond 10 km. Test data includes 3 controlled slow movers with approximately 1 m/s velocity. An example SAR image on which targets are marked is shown in Fig.2. Test site includes discrete clutter sources and road-soil boundaries.
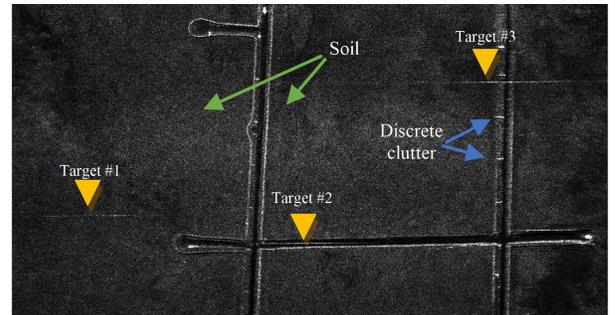


Fig. 2. Test SAR image acquired with SARPER™.

### B. Proposed DP-TBD Algorithm Application

Determining $H_1$ and $H_0$ hypotheses models forms the basis of the DP-TBD algorithm. The implementation illustrated in

Fig.1 utilizes pixel intensities in each time column as target measurements. Therefore, features of the target present and target not present cases can be deduced from the corresponding pixel intensities.

The test SAR image given in Fig.2 shows the amplitude of the complex reflectivity. Amplitude measurement models of $H_1$ and $H_0$ hypotheses used in this work are based on both a priori knowledge and test data observations. $H_0$ hypothesis model is determined as follows: Test image shown in Fig.2 is a high resolution heavily speckled SAR image. The speckle noise of this kind is best represented via multi parameter distributions to handle both contrast and mean intensity [19]. Different distributions are proposed in the literature in this sense such as log-normal, gamma, K-distribution [19], [20]. The best fit is determined from the test data as a gamma distribution. Homogeneous areas of the test SAR image determined by visual inspection are used to determine the best model fit with approximately 50000 sample pixels. Fig.3 and Fig.4 show the distribution fitting results to the logarithm of gamma distribution, which is defined as:

$$\log(f_g(x|a,b)) = -a \log(b) - \log(\Gamma(a)) + (a-1)\log(x) - \frac{x}{b} \tag{3}$$

where $a$ and $b$ are the two parameters of the gamma distribution. $\Gamma(.)$ is the Gamma function.

The distribution parameters, i.e., the fitted shape ($a$) and scale ($b$) parameters, are $a = 2.88$, $b = 0.50$ and $a = 2.68$, $b = 0.44$, for the clutter data samples collected from two different areas shown in Fig.3 and Fig.4, respectively.

Similar to the clutter intensity pdf estimation, the target intensity pdf can be estimated by considering cumulative behavior of the target containing cells. To this end, the signature of a moving target in the SAR image needs to be analyzed. The moving targets have line-like signatures in the SAR images as shown in the test SAR image given in Fig.2. The phase errors resulting from uncompensated target motion smear and displace the target signature in along track direction [21], [22], [23]. The displaced moving target signature effect is known as the "Train of the Track Effect". The extents of the displacement and smearing depend on the target velocity and acceleration. The line-like trail smears also in the cross track direction due to the residual range migration of the target after the range migration correction. The extent of the smear in the cross track direction is much shorter than that in the along track direction which constitutes the line-like-form.

A priori knowledge of the expected line-like rectangular shaped target signature in the SAR image is used to build the target intensity model. The expected signature is nearly a rectangle whose width is within 3-10 pixels (in rows) and length is within 100-300 pixels (in columns) in the tested SAR image. The pixel intensities within this rectangle show slow variation. Transitions between background and target pixels are visible on the image which means that pixel intensities abruptly change at the transitions. Therefore, as a target intensity model Gaussian pdf with a small variance about the
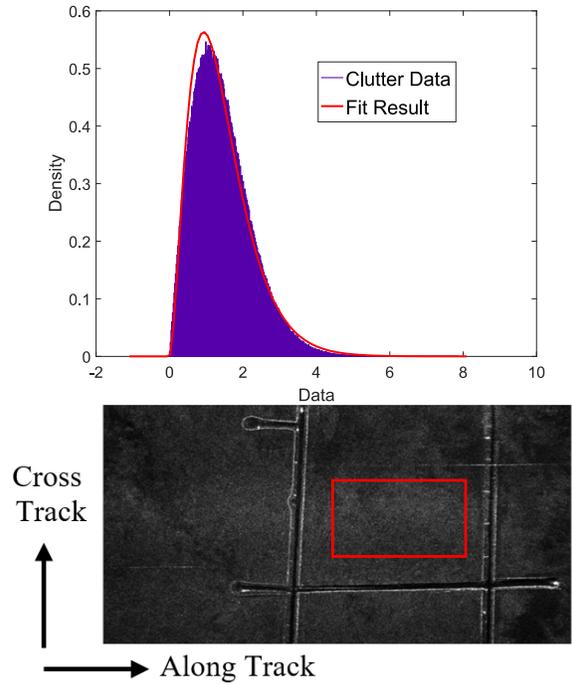


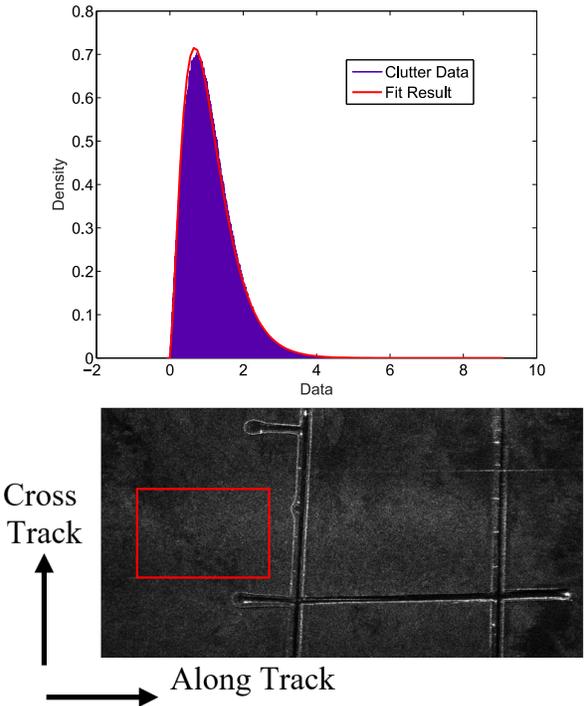Fig. 3. Sample area 1 and the associated intensity pdf.



Fig. 4. Sample area 2 and the associated intensity pdf.

mean corresponding to the average target pixel intensity is used. The logarithm of Gaussian pdf is given as:

$$\log(f_n(x|\mu,\sigma)) = -\frac{\log(2\pi\sigma^2)}{2} - \frac{(x-\mu)^2}{2\sigma^2} \tag{4}$$

where $\mu$ and $\sigma$ are the mean and standard deviation of the normal distribution, respectively.

The optimum width of the rectangular target model deduced from the data is 5 pixels considering the smear in the cross track direction. Hence log likelihood ratio of the cell $j_k$ is constructed from pixel intensities $Y_k$ of the pixels $\{j_k - 2, j_k, j_k + 2\}$ as follows:

$$l_k(j_k) = \begin{cases} H_0 : \log(f_c(Y_k(j_k + 2))f_c(Y_k(j_k))f_c(Y_k(j_k - 2)) \\ H_1 : \log(f_c(Y_k(j_k + 2))f_t(Y_k(j_k))f_c(Y_k(j_k - 2)) \end{cases}$$
$$(5)$$

where $f_c(.)$ denotes clutter intensity pdf and $f_t(.)$ denotes target intensity pdf. This model takes into account that the searched trajectory is line-like and allowable transitions are up to 2 pixels. The likelihood of hypothesis $H_1$ in (5) becomes large if the intensity of the cell of interest fits the target intensity pdf while the intensities of the cells which are 2 pixels apart fit the clutter intensity pdf. $H_0$ hypothesis, on the other hand, requires that both the cell of interest and the cells which are 2 pixels apart fit the clutter intensity pdf.

The smear in the cross track direction of the target signature is also used to determine the transition pdf. Transition pdf is assigned considering the expected trajectory of the target in the image, i.e., line-like signatures. Therefore, no transitions are allowed between image cells which are more than 2 pixels apart as illustrated in Fig.1. The transition pdf used in this work is determined as:

$$p(j_k|j_{k-1}) = \begin{cases} \alpha, & j_k - j_{k-1} = 0 \\ \beta, & j_k - j_{k-1} = \mp 1 \\ \gamma, & j_k - j_{k-1} = \mp 2 \\ 0, & \text{otherwise} \end{cases}$$
$$(6)$$

where $\gamma < \beta < \alpha$. These values in the transition pdf ensures that the transition to the cell in the same row is the most likely while the likelihood decreases with the distance. Note that the transition to a cell which is more than 2 pixels apart is not allowed. Restrictive transition costs (assigning zero probability for some transitions) are applicable when the target trajectory has deterministic restrictions, as in moving target signatures in the SAR images [15].

Due to the possibility of multiple targets in the SAR image, we introduce modifications in (1). Transitions between target pixels and background pixels have a serious effect on the $LPR$ values. The long trail of the target signature in the along track direction (time) causes gradual accumulation of $LPR$ towards the end of the trail. When the target signature is over, the accumulated likelihood ratio cannot decay sufficiently rapidly in time resulting in clutter pixels having high $LPR$ values which might exceed the threshold. To reduce the accumulation of $LPR$ values, a forgetting factor, $0 < \lambda < 1$, is introduced as follows:

$$LPR_k^*(j_k) = l_k(j_k) + \lambda \max_{j_{k-1}}[\log(p(j_k|j_{k-1}) + LPR_{k-1}^*(j_{k-1})]$$
$$(7)$$

where the maximum of the prior state score is weighted with the factor $\lambda$ so that past $LPR$ values are forgotten. Furthermore, to prevent $LPR$ values from getting too large during iterations, when $LPR$ values exceeds a threshold $\eta$ it is reset to $\eta > 0$. Similarly, $LPR$ values might become very low throughout the consecutive background pixels. This may cause a delay in target detection when a switch occurs from background pixels to target pixels. To overcome this, $LPR$ is limited from below to $-\eta$. As a result, $LPR$ values are hard-limited to interval $[-\eta, \eta]$.

## III. RESULTS

### A. Simulation Results

Before moving on to the real data results, the algorithm is tested on simulated data. Four different targets with Gaussian pdf are modelled with additive normally distributed noise background to analyze the behavior of the algorithm. The parameters used in simulations are given in TABLE I.

TABLE I
SIMULATION PARAMETERS

| Parameter | Value | Description |
|---|---|---|
| $\log(f_t(.))$ | $f_n(x|4, 2)$ | Logarithmic target intensity pdf |
| $\log(f_c(.))$ | $f_n(x|1, 1)$ | Logarithmic clutter intensity pdf |
| $p(j_k|j_{k-1})$ | $\alpha$=0.9 $\beta$=0.05 $\gamma$= 0.001 | Transition pdf |
| $\lambda$ | 0.99 | Forgetting factor |
| $\eta$ | 5 | Threshold |

The target intensity pdf, transition pdf and forgetting factor are selected as the ones used in the real data. On the other hand, the background pdf model is selected as a normal distribution (4) with $\mu = 1$, $\sigma = 1$. The threshold $\eta$ is adjusted considering the characteristics of the simulated data. Monte Carlo (MC) simulations are carried out 1000 times. In each MC run noise and target realizations are obtained with the same density parameters. The two different realizations of the simulated data are shown in Fig.5.

The simulated background data has dimensions of $250 \times 250$ pixels. Target signatures are modelled as $5 \times 51$ pixel sized vectors with Gaussian pdf with parameters given in TABLE I. Main targets to be detected are targets 1, 3, and 4. Target 2 is the control target whose main purpose is to observe the effect of target intensity pdf mismatch. DP algorithm is run on the simulated images and the resulting detection probabilities are given for different parameter selections in TABLE II. The false alarm probability, which is defined as the ratio of detected false alarm pixels to the total clutter pixels, is 0.79 %.

TABLE II
TARGET PARAMETERS

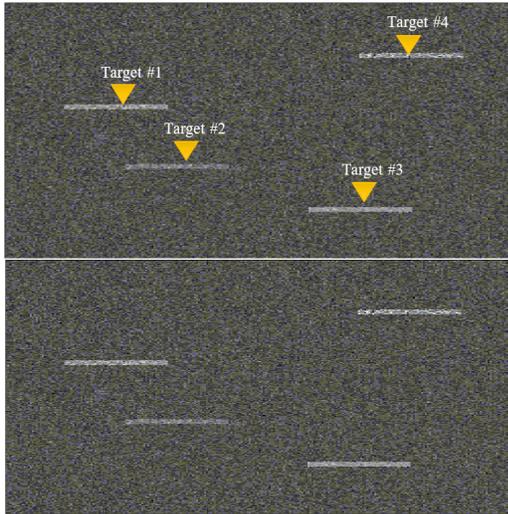| Target No | PDF Parameters | Detection Probability |
|---|---|---|
| 1 | $\mu = 4$ ; $\sigma^2 = 2$ | 97.77 % |
| 2 | $\mu = 2.5$ ; $\sigma^2 = 2$ | 45.13 % |
| 3 | $\mu = 4$ ; $\sigma^2 = 5$ | 91.17 % |
| 4 | $\mu = 4$ ; $\sigma^2 = 1$ | 99.04 % |

Fig. 5. Simulated data realizations.

Another set of simulations is carried out by changing background pdf $f_c(\cdot)$ parameters used by the DP algorithm to $\mu = 1$, $\sigma = 2$ with the same Monte Carlo data-set (Hence there is a mismatch between the data and the parameters used in the DP algorithm). The results are given in TABLE III. The false alarm probability is 1.02 %.

TABLE III
CASE OF VARIANCE MISMATCH IN $H_0$ HYPOTHESIS

| Target No | PDF Parameters | Detection Probability |
|---|---|---|
| 1 | $\mu = 4$ ; $\sigma^2 = 2$ | 99.80 % |
| 2 | $\mu = 2.5$ ; $\sigma^2 = 2$ | 85.28% |
| 3 | $\mu = 4$ ; $\sigma^2 = 5$ | 97.89 % |
| 4 | $\mu = 4$ ; $\sigma^2 = 1$ | 99.99 % |

A final set of simulations is carried out by changing background pdf $f_c(\cdot)$ parameters used by the DP algorithm to $\mu = 2$, $\sigma = 1$ with the same Monte Carlo data-set, i.e., a mismatch in the mean value for the clutter hypothesis. The results are given in TABLE IV. The false alarm probability is 0.70 %.

TABLE IV
CASE OF MEAN MISMATCH IN $H_0$ HYPOTHESIS

| Target No | PDF Parameters | Detection Probability |
|---|---|---|
| 1 | $\mu = 4$ ; $\sigma^2 = 2$ | 93.96 % |
| 2 | $\mu = 2.5$ ; $\sigma^2 = 2$ | 0 % |
| 3 | $\mu = 4$ ; $\sigma^2 = 5$ | 89.43 % |
| 4 | $\mu = 4$ ; $\sigma^2 = 1$ | 95.20 % |

The presented results show that the detection performance is heavily influenced by the target model mismatch. TABLE II and TABLE III show high probability of detection rates for Target 1, 3 and 4. The reason is that these targets are in good agreement with the target intensity pdf. Variance mismatch of the clutter intensity pdf results in higher false alarm rate than

the case of no clutter intensity pdf model mismatch. TABLE IV shows lower detection probabilities for all targets as the clutter intensity pdf becomes similar to target intensity pdf. Target 2 has the lowest detection rate since the gap between the target intensity pdf and the clutter intensity pdf is the smallest in this case.

As a result of this experiment we can conclude that if the parameters of $H_1$ is relatively close to the true target behavior and the background pdf is homogeneous throughout the image, the proposed approach is expected to give satisfactory results.

### B. Real Test Data Results

The proposed method is applied on an actual SAR image containing slow moving targets. The parameters used in this experiment are given in TABLE V.

TABLE V
PARAMETERS UTILIZED FOR THE FIELD EXPERIMENT

| Parameter | Value | Description |
|---|---|---|
| $\log(f_t(.))$ | $f_n(x|4, 2)$ | Logarithmic target intensity pdf |
| $\log(f_c(.))$ | $f_g(x|2.8, 0.5)$ | Logarithmic clutter intensity pdf |
| $p(j_k|j_{k-1})$ | $\alpha$=0.9 $\beta$=0.05 $\gamma$= 0.001 | Transition pdf |
| $\lambda$ | 0.99 | Forgetting factor |
| $\eta$ | 180 | Threshold |

$LPR$ score surface obtained is given in Fig.6. In the figure it is shown that target $LPR$ scores rise towards the center of the target signature and they gradually decrease towards the end as expected. Since the search is for the line-like trajectories in SAR image, some other similar segments of the image with the similar features, i.e., false alarms, are also captured.

To see the detections whose $LPR$ scores exceed the threshold, a 2 dimensional CFAR filter is implemented. One dimensional guard cells and threshold cells in the conventional CFAR are replaced with cells in a rectangular form. Similar to the conventional method, a CFAR threshold is estimated from the neighboring cells. The illustration is given in Fig.7.

$LPR$ scores after thresholding are shown in Fig.8 where detections are marked in green color. This shows that 3 controlled targets are detected with a few false alarms due to the line-like background features in the image.

### IV. CONCLUSION

The implementation of a dynamic programming based sequence detection method, namely DP-TBD method, to the slow moving target detection on SAR image problem is presented with real data results. The method is customized to capture the line-like signatures of the moving targets on the SAR image. The results show that the tracker is capable of determining the target signatures with few false alarms in the test data including road-soil boundaries some of which form line-like features, discrete clutter sources and speckle. Although the measurement models for the background and target together with some parameters such as $\eta$ are dependent
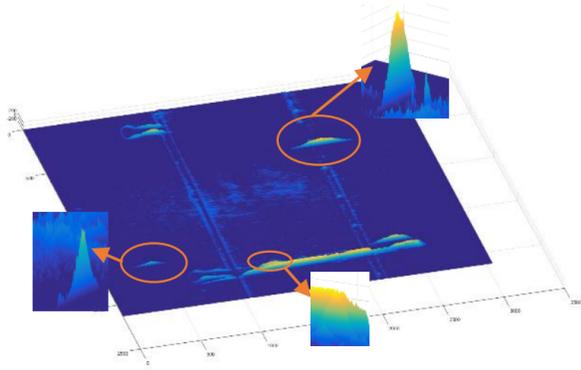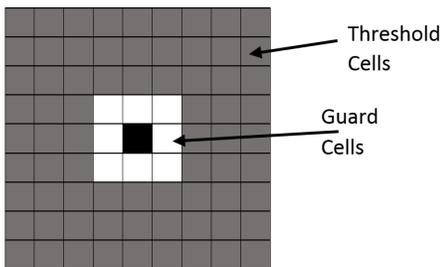
Fig. 6. *LPR* score surface.



Fig. 7. 2-D CFAR illustration.



Fig. 8. *LPR* after thresholding.

on the characteristics of the data at hand, proper estimation of these through the observations leads to successful results.

The method does not provide further information regarding the target (e.g., velocity, direction) at this stage. Future work on this subject may focus on extracting target specific information once a detection is made. Estimating target velocity components through the detected target signature can be possible. Alternatively moving target focusing methods can be applied on the detected targets. Such methods are computationally demanding when applied to the whole image data.

## ACKNOWLEDGMENT

## REFERENCES

[1] J. S. Goldstein, M. L. Picciolo, M. Rangaswamy, and J. D. Griesbach, "Detection of dismounts using synthetic aperture radar," in *IEEE Radar Conference*, 2010, pp. 209–214.

[2] O. R. Fogle and B. D. Rigling, "Dismount feature extraction from circular synthetic aperture radar data," in *IEEE Radar Conference*, 2012, pp. 0122–0127.

[3] J. R. Fienup, "Detecting moving targets in SAR imagery by focusing," *IEEE Transactions on Aerospace and Electronic Systems*, vol. 37, no. 3, pp. 794–809, 2001.

[4] K. Y. Li, F. Uysal, S. U. Pillai, and L. J. Moore, "Modified space time adaptive processing for dismount detection using synthetic aperture radar," in *IEEE Radar Conference*, 2012.

[5] A. K. Naima Amrouche and D. Berkani, "Multiple target tracking using track before detect algorithm," in *International Conference on Electromagnetics in Advanced Applications (ICEAA)*, 2017, pp. 692–695.
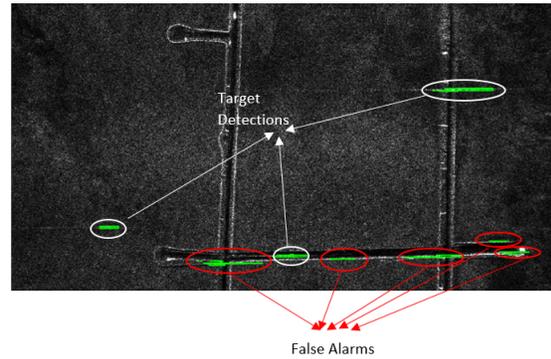
[6] G. J. Huang Yong, "A track-before-detect algorithm for statistical MIMO radar multitarget detection," in *IEEE Radar Conference*, 2010, pp. 12–16.

[7] M. Eyili, "Multi-target particle filter based track before detect algorithms for spawning targets," Master's thesis, Middle East Technical University, 2014.

[8] M. Sabuncu, "Particle filter based track before detect algorithm for tracking of dim moving targets," Master's thesis, Middle East Technical University, 2012.

[9] L. R. Moyer, J. Spak, and P. Lamanna, "A multi-dimensional Hough transform-based track-before-detect technique for detecting weak targets in strong clutter backgrounds," *IEEE Transactions on Aerospace and Electronic Systems*, vol. 47, no. 4, pp. 3062–3068, 2011.

[10] G. Sahin and M. Demirekler, "A multidimensional Hough transform algorithm based on unscented transform as a track before detect method," in *IEEE 17th International Conference on Information Fusion*, 2014, pp. 1–8.

[11] Z. Wang and J. Sun, "Maneuvering target tracking via dynamic programming based track before detect algorithm," in *CIE International Conference on Radar*, 2016, pp. 1–4.

[12] W. Yi, L. Kong, J. Yang, and X. Deng, "A tracking approach based on dynamic programming track before detect," in *IEEE Radar Conference*, 2009, pp. 1–4.

[13] F. Gao, F. Zhang, H. Zhu, J. Sun, and J. Wang, "An improved TBD algorithm based on dynamic programming for dim SAR target detection," in *12 th International Conference on Signal Processing*, 2014, pp. 1880–1884.

[14] E. L. Melita Hadzagic, Hannah Michalska, "Track-before detect methods in tracking low-observable targets: a survey," *Sensors Trans Magazine*, vol. 54, no. 1, pp. 374–380, 2005.

[15] R. G. Gallager, *Stochastic Processes: Theory for Applications*. Cambridge University Press, 2013.

[16] H. P. James Arnold, S.W. Shaw, "Efficient target tracking using dynamic programming," *IEEE Transactions on Aerospace and Electronic Systems*, vol. 29, no. 1, pp. 44–56, 1993.

[17] Z. F. H. Askar and Z. Li, "Detecting dim moving point targets using transformation of pixel statistic," in *IEEE Internationa Conference on Communications, Circuits and Systems and West Sino Expositions.*, 2002, pp. 972–976.

[18] "Sarper$^{TM}$ online," 2018, http://www.aselsan.com.tr/en-us/capabilities/radar-systems.

[19] C. Oliver and S. Quegan, *Understanding Synthetic Aperture Radar Images*. SciTech Publishing, 2004.

[20] A. C. Frery, H. J. Muller, C. Yanasse, and S. Sant'Anna, "A model for extremely heterogeneous clutter," *IEEE Transactions on Geoscience and Remote Sensing*, vol. 35, no. 3, pp. 648–659, 1997.

[21] J. Raney, "Synthetic aperture radar and moving targets." *IEEE Transactions on Aerospace and Electronic Systems*, vol. 7, no. 3, pp. 499–505, 1971.

[22] M. Soumekh, *Synthetic Aperture Radar Signal Processing*. New York: Wiley, 1999.

[23] G. K. Stefan V. Baumgartner, *Multi-Channel SAR for Ground Moving Target Indication*. Elsevier, 2014.